COMPARING THE EFFECTS OF PROTECTIVE PLATE SHAPE ON LEG INJURIES DURING FINITE ELEMENT BLAST SIMULATIONS WITH THE HYBRID III ATD

A Senior Thesis

Submitted to the Engineering Honors Program

Of the University of Notre Dame

In Partial Fulfillment of the Requirements

For the Degree of

Bachelor of Science in Aerospace Engineering

by

Teresa A. Henisey

_____

Andrés Tovar, Advisor

Engineering Honors Program

Notre Dame, Indiana

November 2010

COMPARING THE EFFECTS OF PROTECTIVE PLATE SHAPE ON LEG INJURIES DURING FINITE ELEMENT BLAST SIMULATIONS WITH THE HYBRID III ATD

Abstract

by

Teresa A. Henisey

This thesis explores leg injuries caused by blasts located underneath military vehicles and compares the effectiveness of different protective panel shapes in simulated blast environments. Four panels with shapes determined by different optimization techniques are affixed to a finite element model of a simplified vehicle. The control shape is flat, and the other three shapes come from Displacement Basis, Gaussian, and Hybrid Cellular Automata optimization algorithms. A model of an Anthropomorphic Test Device is imported into the set-up and arranged into a typical seated position.

The ConWep function in LS-PrePost is applied to the bottom surface of the plates to represent a typical road mine. LS-DYNA mathematically calculates the loads on the surface using a loading function that does not incorporate the effects of the surroundings. The original designers of the simplified vehicle and plate model (Williams et al., 2003)

validated the accuracy and applicability of the ConWep design to represent a physical model.

The analysis focuses on leg injuries. Leg injuries are some of the most common and harmful injuries associated with blasts. Loading on the tibia and femur are calculated using LS-PrePost and compared to critical limit standards to estimate the possibility and severity of injury.

The Displacement Basis plate performs the best in this experiment. Furthermore, all of the three modified plates offer more protection than the flat plate. The main variable that leads to the success of the Displacement Basis plate is the minimal distance the plate penetrates into the vehicle cabin. It retains its parabolic shape and does not snap through to enter the cabin. Thus, it does not make contact with the feet of the occupant.

The limitations of this research stem from the inability of ConWep to account for the compounding effects of air and soil. Both can exacerbate the severity of injuries by creating a pressure wave and redirecting blast energy, respectively. However, this drawback can be accounted for by increasing the mass of the explosive material during simulations.

CONTENTS

LIST OF TABLES

LIST OF FIGURES

ACKNOWLEDGMENTS

I am grateful for my advisor, Dr. Andrés Tovar, for giving me the opportunity to research with the Design Automation Laboratory. His efforts provided me with the funding that made my undergraduate research possible. The summer I spent researching under him was an incredibly productive, educational, and enjoyable time.

Also, I appreciate the efforts of Dr. John E. Renaud and the members of the committee, Dr. Stephen Batill and Dr. Karel Matous. Additionally, the Engineering Honors Program staff, especially Dr. Bill Goodwine, made my project possible through their contributions to undergraduate research.

Lastly, I would also like to thank the entire Design Automation group, particularly Juan Camilo Medina, Andy Baumann, Kyle Kinnary, Huade Tan, and Chandan Mozumder. They were excellent sources of information and enthusiastic teammates. Huade Tan was especially patient, helpful, and my go-to person for all of my many questions.

ABBREVIATIONS

AIS	Abbreviated Injury Scale
ALE	Arbitrary Lagrangian Eulerian
ATD	Anthropomorphic Test Device
DAL	Design Automation Laboratory
DRDC	Defense Research and Development Canada
FEM	Finite Element Model
GM	General Motors
HCA	Hybrid Cellular Automata
IED	Improvised Explosive Device
IIHS	Insurance Institute for Highway Safety
LSTC	Livermore Software Technology Corporation
MRAP	Mine Resistant Ambush Protected
NHTSA	National Highway and Traffic Safety Administration
PPE	Personal Protective Equipment
RCC	Research Computing and Cyberinfrastructure
RHA	Rolled Homogenous Armor
TI	Tibia Index

CHAPTER 1:

INTRODUCTION

1.1 Justification

In the most recent war in the Middle East, explosions from road mines and improvised explosive devices (IEDs) were behind over 60 % of the fatalities among American troops in Iraq and over 50 % in Afghanistan (Defense Manpower Data Center, 2010). More than 27,000 troops were killed or wounded by roadside and car bombs. Military vehicles were the primary target of these bombs and mines. Protecting the vehicles from blasts has the potential to save thousands of lives each year.

Legs sustain the most numerous and life threatening injuries during vehicular explosions (van der Horst et al., 2005). The high risk for leg injury in anti-tank and vehicle explosions stems from one main reason. IEDs and mines buried under roads are triggered either automatically or remotely as a vehicle drives over it. Therefore, the underside of the vehicle absorbs most of the energy from the blast. The floor panel in these vehicles can deform, accelerate upward, and even tear apart. Feet and lower legs are the closest body parts to the floor and also the closest to the blast itself. Thus, lower leg injuries are the most prevalent injury. Though not necessarily fatal, severe leg injuries can cause death especially in battlefield environments when medical attention is not readily available. Also, legs injuries are the leading cause for loss of life years

(Kuppa et al., 2001). Loss of mobility is an enormous detriment to the lives of the victims and a costly and lengthy process to treat. Designing vehicles and devices to prevent lower leg injury is crucial for the safety of deployed personnel in heavily mined areas.

However, testing protective equipment poses a challenge due to the dangerous and destructive nature of blasts. Computer simulations are possible substitutes for physical testing. A program with the ability to simulate a vehicular blast and its effects on occupants could provide data without endangering human lives.

1.2 Theoretical Research

Many blast-related injuries arise from the interplay between a vehicle and its occupants. Typically these injuries can be classified as secondary or tertiary effects of explosions (Stuhmiller, 2008). Secondary effects are injuries caused by the impact of debris and blast material that were set in motion by the blast. The interaction of the accelerated floor and stationary feet is an example of a secondary effect. Tertiary effects are impacts caused from the acceleration of the body. An accelerated body can strike a wall, the ground, or the ceiling of a vehicle.

Currently, the Humvee, a staple for military transportation in deployed areas, is highly targeted by road mines and IEDs. Their low ground clearance, low weight, and flat undersides are conducive to absorbing blast energy and offering little protection (Eisler et al., 2007). The military has developed the Mine Resistant Ambush Protected (MRAP) vehicle that offers more protection, but these multimillion dollar vehicles are

limited and cannot replace the thousands of Humvees stationed in dangerous areas. One alternative is retrofitting the traditional Humvees with additional blast protection.

Many improvements have already been made in the field of blast protection. Personal protective equipment (PPE) and ballistic blankets have been implemented to protect against firearms and shrapnel. Unfortunately, they have proven to be ineffective in close proximity to large explosions (Durocher, 2003). Other devices, such as blast plates and armor, are much more effective at protecting occupants from powerful blasts. These inventions are typically comprised of composite foams and strengthened metals that absorb or deflect blast energy. Though effective, this type of armor is incredibly heavy. Additional ballistic protection can add up to 2000 kg to a vehicle. Most light vehicles do not have the structural strength to accommodate such a protection system (Durocher, 2003). Also, the extra weight affects stability. Components, such as braking and steering, are unsuited for the added load (Grujicic et al., 2009). Therefore, a design that protects occupants while adding only minimal weight is ideal.

One option to increase blast protection without increasing weight is to experiment with the shape of preexisting protective panels. In this way, additional weight is minimal. Current protection can just be adapted to be the optimal shape for blast deflection and absorption. Deflection refers to the redirection of blast energy away from occupants, while absorption means the structure absorbs the energy without transferring it to the occupants. Some shapes deflect and absorb blast energy much more effectively than a typical flat plate of the same material.

While testing actual structures under blast loads can give some insight into its protective qualities, a stand-in for an occupant must be incorporated into the system to

study the effects of the environment on the occupant. This stand-in occupant needs to closely mirror actual human anatomy and produce measureable data under potentially destructive conditions.

Anthropomorphic Test Devices (ATDs), more commonly known as crash test dummies, are the ideal candidates for blast testing. They closely resemble the human body and can be used in harmful testing conditions. Most dummies are designed to be as tall as and weigh as much as the average male. These devices even react to applied loads in a similar way as the human body. The complex system is described as biofidelic, meaning that it mirrors human anatomy (Bellis, 2009).

Dummies have become more advanced and biofidelic in recent decades in order to meet the demands of the ever expanding crash test industry. The first crash test dummy was Sierra Sam, commissioned in 1949 by the US Air Force for testing pilot ejection seats. He was much heavier and bulkier than the average human. His inventor, Samuel W. Alderson, later adapted this model to be used in both aircraft and motor vehicle crash testing.

Crash test dummies did not begin to resemble the actual weight and height of the average man until 1971 when General Motors (GM) introduced the Hybrid I, a combination of the best features of two leading dummies, the VIP-50 series and Sierra Stan. Due to its uniquely average design, it became known as the 50^{th} percentile male dummy. Hybrid II was released a year later with improvements that complied with the American Federal Motor Vehicle Safety Standards.

The Hybrid family was a considerable improvement over cadaver and early dummy testing. Namely, it was standardized so crash conditions could be replicated with

similar results. Cadaver testing and early dummies would produce singular results that were difficult to replicate since each test subject was unique (Wikipedia, 2010). Despite Hybrid II's advantage, it still lacked accuracy. The design did not reflect the stiffness of actual human biomechanical data or include the response of internal body components. These defects limited it mainly to testing seatbelt effectiveness (Bellis, 2009).

To correct these errors, GM released the Hybrid III in 1977. It is 1.72 m tall when standing, 0.88 m tall when sitting, and weighs 78 kg, the proportions of the 50^{th} percentile male (HFM-090 Task Group 25, 2007). It has 44 data channels throughout its body that record acceleration, displacement, and force. It has realistic leather-like skin, a bendable, stretchable neck, and even a steel rib cage. Its resemblance to the human body, in terms of weight, joint stiffness, geometry, and energy absorption, means it reacts in a similar way as actual humans when subjected to a traumatic environment (Noureddine et al., 2002). Moreover, the accuracy of its numerous data channels allows the Hybrid III to effectively demonstrate occupant injury in more complex crash situations, including airbags and multiple vehicle crashes.

The most notable advantage of the Hybrid III crash test dummy is its standardization. It can be used multiple times. Also, the dummy consists of entirely replaceable parts. Meaning, if one part of the dummy broke, it can simply be replaced without having to buy a whole new dummy. This in turn standardizes the results of testing done on dummies. Different dummies subjected to the same loading will measure similar results.

The superiority of the Hybrid III has been recognized by the National Highway and Traffic Safety Administration (NHTSA). It is currently the mandated dummy for

federal regulations and NHTSA's motor vehicle safety standards, as noted in the Code of Federal Regulations under Title 49, Part 572, Subpart E.

The Hybrid III dummy is most commonly used for frontal car crash testing. However, the Hybrid III has been validated for blast testing with detonations under the vehicle or when the dummy is shielded from the direct blast and the effects of overpressure. The dummy is loaded via vehicle deformation and acceleration in a similar way that dummies are loaded in crash testing. Physical testing and computer simulations have proven the effectiveness of using the Hybrid III dummy in blast testing (van der Horst et al., 2005).

Due to its accuracy, a dummy has not been developed for use primarily in blast tests. This is in part a reflection of the versatility of the Hybrid III and also of the relatively limited demand for blast testing. Crash testing is much more common because of the large and public demand for safer cars, whereas only the military regularly encounters blasts (Chichester et al., 2001). Most blast testing research has been done in partnership with either the United States military or Canadian defense development. Therefore, the vehicles and materials used in blast testing are those commonly found in war environments.

The main shortcoming of using the Hybrid III for blast testing is its inability to measure the effects of blast overpressure. Blast overpressure is defined as the region directly in front of a blast wave with pressures exceeding atmospheric levels. The compression of the air in this region heats and accelerates the air molecules (Mayorga, 1997). In certain instances, the effects of overpressure can be neglected during blast testing. Since the majority of research applies blasts to vehicles, the components of the

vehicle block the air blast associated with overpressure. If cracks and fissures are present in the structure, then the dangerous effects of overpressure must be taken into account. For the tests run in this project, the floor panel is assumed to have no openings and the occupant is protected from the harmful pressure gradient. Though possible, it is more complex to study the effects of blast overpressure in physical tests. A dummy must be fitted with an additional pressure device that is strapped around its chest to determine the effects of overpressure on the lungs, thorax, and trachea (HFM-090 Task Group 25, 2007). These lengths are not necessary for this research.

A secondary drawback to the Hybrid III is its large price tag. With a cost of over one hundred thousand dollars (Nelson et al., 1996), the Hybrid III is an expensive tool to use in highly dangerous and potentially destructive environments. While they were designed to last through multiple crash tests, they may not be able to survive the heat, loading, and overpressure from a large explosion. On a similar note, blast testing poses serious risk to the researchers in the vicinity, especially when simulating a detonation on the scale of those used in wartime situations. Blast testing incurs large risks and overwhelming financial costs.

An alternative to actual blasts are virtual blasts. Finite-element modeling (FEM) is significantly faster, cheaper, and safer than traditional experiments. Finite-element modeling also makes it easier to acquire data. A node can simply be selected and analyzed as opposed to having to incorporate complex measurement devices. In many cases, virtual models are just as accurate as actual tests.

LS-DYNA is a dynamic finite-element software that can accurately simulate the complex processes and movement associated with a blast. Furthermore, LS-DYNA

incorporates ATD finite-element models, including the Hybrid III 50th percentile male, 50th percentile female, 95th percentile male, side impact dummy, and BioRID (LSTC, 2010). LS-PrePost, a user interface for creating and analyzing models along with LS-DYNA, is employed for all pre- and post-processing due to its compatibility with ATD models and easily accessible ConWep function.

The state-of-the art advancements in ATDs and virtual simulations result in a safe, fast, and realistic blast test. With these tools, structures can be subjected to blasts similar to those detonated by enemy forces, and the harmful effects on occupants can be assessed. In this way, different protection options can be compared to determine the most effective way to protect against blast related injuries.

The Design Automation Laboratory (DAL) at the University of Notre Dame focuses in part on designing blast protection. It couples LS-DYNA with structural optimization algorithms to design blast mitigating plates (Tan et al., 2010d). Three main optimization techniques used for plate design are Displacement Basis, Gaussian, and Hybrid Cellular Automaton (HCA) (Tan et al., 2010d). These algorithms were designed to minimize nodal acceleration. However, optimized protection has not been tested in simulations with ATDs, which could retrieve occupant injury data. The actual protective effects of these plates on vehicle occupants have not been compared.

1.3 Objectives

The objective of this research is to evaluate the protective capabilities of blast mitigating plates by comparing occupant injury data. The four main plates of interest are a flat plate and three designed by the DAL: Gaussian, HCA, and Displacement Basis.

This broad goal is narrowed down to a set of smaller tasks. First, an appropriate dummy is selected to represent an occupant. Second, a simplified model of a military vehicle is designed. Third, the occupant is imported into the model. Fourth, a blast is simulated and results are assessed. Acquired data focuses on leg injury caused by an accelerating floor. The forces and moments on the tibia and femur are measured and compared against critical values to determine the possibility and severity of injury. Also, the displacement, velocity, and acceleration of the protective plates are recorded to determine the primary variable linked to injury. The process is repeated with four different panel shapes to compare protection offered and primary causes of injuries.

CHAPTER 2:

ANTHROPOMORPHIC TEST DEVICES

2.1 Injury Criteria for the Hybrid III ATD

The Hybrid III ATD is designed to replicate a human response, but determining the extent of simulated injuries inflicted during a test is not always obvious. Therefore, certain criteria levels have been determined to signify when an injury is likely to occur. These critical values and indices were calculated based on actual injury observation, cadaver testing, and crash test dummy evaluations.

Cadaver based results often vary since every human body is different. This explains the variation between sources of what critical values should be used. The ones given below in Table 1 and depicted in Figure 1 are the most common criteria used among researchers and also the most applicable for the research focused on leg injury. These values are appropriate for assessing leg injury using the Hybrid III ATD. They also mark the minimum values for a marginal rating or the limit when fractures become likely. This is defined on the Abbreviated Injury Scale (AIS) as AIS 2+. The scale varies from 1, no injury, to 6, fatal. A score of 2+ means the injury is moderate at best.

Table 1:

Injury assessment values for the leg (Mertz, 1993; Kuppa et al., 2001)

Parameter	50th Percentile Male Dummy
Critical Tibia Compressive Force (F_c)	35.9 kN
Critical Tibia Bending Moment (M_c)	225 N•m
Tibia Index	1
Tibia Axial Force (Compression)	8 kN
Femur Axial Force (Compression)	10 kN
Tibia Axial Force for Ankle injuries (Compression)	6.8 kN

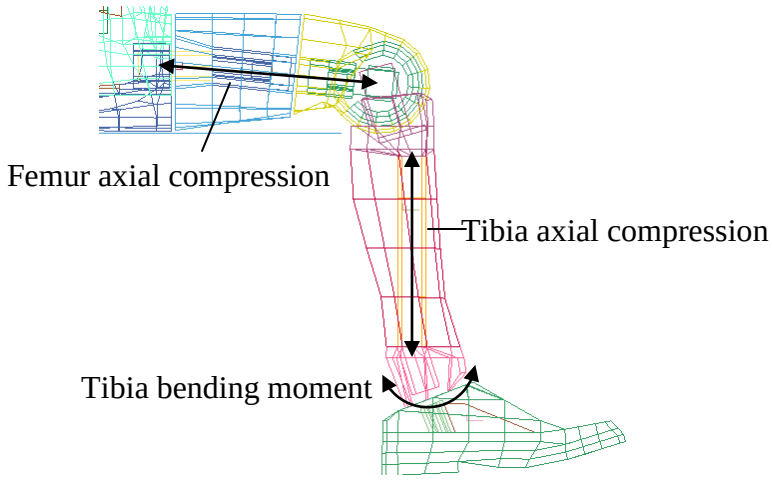

Figure 1: Depiction of injury criteria

To correctly determine the tibia index, the measured tibia bending moments about the Y axis must be corrected before assessing injury since the geometry of the Hybrid III leg does not bend in a biofidelic manner. Purely compressive forces can cause the Hybrid tibia to bend forward, about the Y axis, misleadingly increasing the moment (IIHS, 2009). The following equation, formulated by Welbourne and Shewchenko (1998), mathematically corrects the moment to reflect the total bending of the tibia. The variable F in all equations represents the measured axial forces with units of kilonewtons.

$$M_{y_{corrected}} = M_y + (0.006402)(1000)F \quad (2.1)$$

LS-PrePost measures corrected tibia bending moments through a theta moment stiffness analysis. The magnitudes of the bending moments are calculated next, and then combined with the measured axial forces to calculate the tibia index. Signs of the two terms in the tibia index equation are adjusted to ensure both fractions are positive:

$$M = (M_y{}^2 + M_x{}^2)^{1/2} \tag{2.2}$$

$$TI = \frac{F}{F_c} + \frac{M}{M_c} < 1 \tag{2.3}$$

where F is the measured tibia axial compressive force in kilonewtons and M is the measured bending moment in Newton meters. A value equal to one delineates between an acceptable and marginal rating. In other words, a value greater than one means there is a high possibility of tibia fracture, an AIS 2+ injury.

For femur injury assessment, the value of 10 kN in compression is a widely accepted critical limit. When compressive forces are measured by devices in a dummy or LS-PrePost they are displayed as negative numbers. Therefore, the peak negative values should be compared against -10 kN.

Notably, injury criteria tend to underestimate the maximum values body parts can withstand. This is due in part to the impact of age on the likelihood of injury. Since cadavers are typically older specimens, the critical values calculated by cadaver testing are conservative and probably lower than that of the average male (van der Horst et al., 2005). In a similar way, certain joints in the Hybrid III ATD, namely the knee-femur complex (Rupp et al., 2003), are stiffer than that of cadavers and the average human. Thus, responses recorded in testing with the dummy are going to be higher and over

shorter impact durations. In other words, the injuries predicted in testing would be worst case scenario. Both these facts are beneficial for using ATDs for blast and crash testing. If designs can be optimized to protect dummies in simulated test environments, then they are likely to perform the same or even better in real world applications.

It is important to remember that these critical values are not guaranteed limits that clearly divide no injury from injury. Cadaver testing has revealed that femurs can break at compressive values far less than 10 kN. Conversely, other legs were loaded with much greater forces and sustained zero injury. These values are simply references points that delineate when injury may be likely. Also, they are meant to be conservative values for the average male at an average age.

2.2 Modeling the Hybrid III in LS-PrePost

Finite element models of ATDs have been incorporated into LS-PrePost and LS-DYNA. LSTC released three dummy models for this research assignment: 50^{th} percentile male, 95^{th} percentile male, and 5^{th} percentile female. These models have all properties and contacts already assigned. A user interface allows for the ATD to be easily positioned in set-ups. Each joint can be rotated separately with constraints that mimic actual human movement.

Also, forces, accelerations, and moments of key joints and body parts are automatically recorded for injury assessment. These values can be filtered and plotted in LS-PrePost. Part, joint, and node identification remains constant with each virtual

dummy, simplifying positioning and post-processing. Table 2 lists notable elements and their respective ID numbers.

Table 2:

Hybrid III ID numbers in LS-PrePost

ID Number	Description	Type
1	Center of skull	Node
24	Left femur	Joint
25	Right femur	Joint
42	Left Tibia	Joint
44	Right Tibia	Joint
66	Left thigh	Part
67	Right thigh	Part
72	Outer pelvis/rear end	Part
73	Left foot	Part
80	Right foot	Part

CHAPTER 3:

INITIAL SET-UP AND BLAST TESTING

3.1 Simple ATD and Blast Scenario

To test the feasibility of importing a dummy into a blast scenario, a simple setup with a rigid seat and fixed plate is modeled. This is not meant to realistically model a blast, but it provides insight into dummy positioning, contact parameters, and blast loading.

The seat is constructed from rigid steel and is fixed in space in order to provide an immovable mount for a dummy. In this way, injuries are limited to the contact between the plate and feet. An aluminum plate with dimensions 1000 × 500 × 20 mm is centered beneath the dummy's feet. The SPC function in LS-DYNA fixes the outer edges of the seat and plate. The properties for the materials and contacts are available in LS-DYNA tutorials (RCC, 2010). The plate is made of aluminum because this is a typical vehicle material, and the seat is steel for its rigidity. Table 3 gives the respective properties for the plate and seat.

Lastly, a 10 kg charge is located 500 mm below the center of the plate. ConWep simulates the blast, and the bottom surface of the plate is selected for application of the blast load. The termination time is 15 ms and the D3Plot time step is 0.1 ms. The simulation is run using LS-DYNA.

Table 3:

Properties for seat and plate setup

	Aluminum Plate	Steel Seat
Material Type	003-Plastic_Kinematic	020-Rigid
Density (kg/mm^3)	2.7×10^{-6}	7.83×10^{-6}
Young's Modulus (Gpa)	69	200
Poisson's Ratio	0.3	0.3
Section Type	Solid	Shell (Thickness = 1 mm)

The next step is to import a Hybrid III model into the simulation. The dummy is rotated and translated so that it rests just above the seat, and the limbs are adjusted to a normal sitting position. The lower arms are rotated 90°, and the legs are left in their preset position. Rigid body one way to rigid body is selected for the contact between the seat and the dummy's thighs and pelvis, parts 66, 67, and 72. These are based on LS-PrePost tutorials (LSTC, 2010). An automatic surface to surface contact with default constraints is created between the feet and blast plate. All other parameters are the same as in the first test. The final setup is displayed in Figure 2.

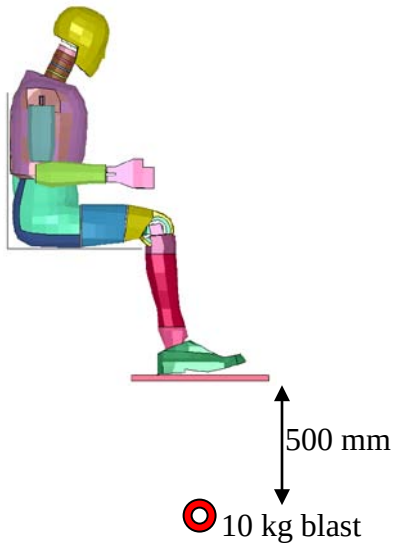

Figure 2: Initial testing setup

An important feature in determining the loading on the legs is filtering the data. Most other research recommends using a Butterworth filter with a filter frequency of 180 Hz (Guha et al., 2008). If too high of a filter frequency is selected, then the data is unreasonably high at its peaks. However, too low a filter underestimates the actual measurements. In these tests, a frequency of 180 Hz produces the most reasonable results. One side effect of using a filter is that the initial value at time t = 0 might not be zero. However, the most important pieces of information are typically the maximum/minimum values so the small offset is not regarded.

3.2 Initial Results

Though the only difference in the test setups is the inclusion of a Hybrid III ATD, the behavior of the blast plate is strikingly different. The maximum deflection of the plate reaches 79 mm in the first test without a dummy but only deforms 9 mm in the second test with the dummy.

The dummy is also severely injured in this blast. The axial femur force reaches 13 kN in compression, 3 kN higher than the critical limit for AIS 2+ injuries. The maximum compressive force and bending moment for the tibias are each approximately three times larger than the respective critical values.

3.3 Initial Conclusions

This extremely simplified test only serves as a baseline for more accurate testing. Though basic, this testing reveals important conclusions. Clearly, the plate transfers most

of the blast energy as shown in the disparities between the two maximum displacements. The dummy's legs absorb this energy, causing severe injuries. Consequently, a plate that absorbs more energy and transfers less energy will protect against leg injuries.

These conclusions provide insight into making further testing more accurate. First, the dummy's feet should not be touching the plate at time t = 0. This causes undue energy transfer where the two parts are intersecting. It is also not realistic, especially when considering curved plates. In real situations, there will likely be carpeting or secondary interior flat plates that suspend the feet slightly above the protective plate. Second, the default settings for the automatic surface to surface contact were insufficient. More energy should have been dissipated due to friction and viscous effects. These changes must be incorporated into further testing to increase accuracy.

CHAPTER 4:

SYSTEM MODEL

4.1 Simplified Vehicle Model and the DRDC Plate

Modeling an entire military vehicle is overly complex especially when only the acceleration of the vehicle floor into the feet is being studied. A simplified version of a cabin floor and protective hull was developed by Williams et al. (2003) for the Defense Research and Development Canada (DRDC). It concentrates the weight of a vehicle into a simple structure over a floor panel. This device was modeled by Tan et al. (2010d) in LS-PrePost.

It consists of a flat plate supported by one stand in each corner. The stands are SAE1020 steel. The visible upper surface of the plate is 4 × 4 ft, or a square with approximately 1,220 mm sides. The plate is 31.75 mm thick and made from AL5083-H131 aluminum. A box beam of the same material as the stand is loaded with an additional 10,620 kg (representing the weight of a light armored vehicle) and sits on top of the plate. The load is divided among mass nodes equally spaced along the box beam. The automatic single surface contact option is used between components. Lastly, only one quarter of the device needs to be modeled as made allowable by the symmetry of the set-up. The quarter plate and its dimensions are depicted in Figure 3.

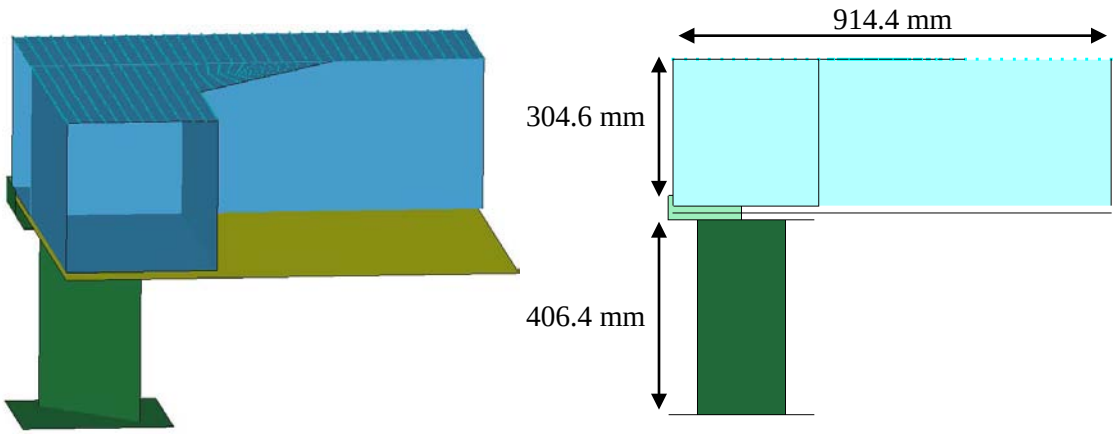

Figure 3: Flat DRDC plate configuration

Aluminum, as mentioned in the initial testing, is common for floor panels. Subsequent testing replaces the aluminum plate with a Rolled Homogenous Armor steel (RHA) plate of the same dimensions. The RHA steel is a stronger yet heavier material developed for blast protection. Table 4 gives the properties of the three materials used in the construction of the device.

Table 4:

Material properties for DRDC plate (Williams et al., 2003)

Property	Steel SAE 1020	Aluminum AL 5083-H131	Steel RHA
Component	Support Frame	Plate	Plate
Density (kg/mm^3)	7.830×10^{-6}	2.768×10^{-6}	7.850×10^{-6}
Elastic Modulus (GPa)	205	70.33	197.5
Poisson's Ratio	0.30	0.33	0.30
Yield Stress (Gpa)	0.350	0.322	1.320
Tangent Modulus (GPa)	0.636	0.340	1.810
Plate Thickness (mm)	12.70	31.75	31.75
Total Mass of Plate (kg)	N/A	73.48	208.396

4.2 ATD Positioning within DRDC Setup

To import an ATD into the set-up, the system first needs to be converted to the ATD's units. The DRDC plate modeled by Tan et al. (2010d) has units of centimeters, grams, 10^7 Newtons, microseconds, and megabars while the ATD is measured in millimeters, kilograms, kilonewtons, milliseconds, and gigapascals.

Next, a seat is required to situate the dummy in the preferred location. The same immovable, rigid seat from initial testing is incorporated into the design. Its fixed and rigid qualities allow it to be stationed independently of the DRDC plate without influencing results. In this way, injuries are caused by only the deforming floor. Also, the seat is located in way that a seated dummy's feet are 30 mm from each edge of the quarter-plate, which places the feet near the center of the full plate. This is almost directly over the blast where the plates deform the most. Essentially, this is modeling a worst case scenario. The dummy's feet are suspended 10 mm over the top surface of the flat plate position. This is preferable to the feet resting directly on the floor. If the feet intersect the plate even minutely, then they would absorb more energy from the plate than realistic as proven during initial testing. Some energy from the plate should be reflected or dissipated.

Also, the feet and the protective plate realistically should be separated by a light cabin floor panel suspended over the armor. Pressure would build between the two plates as the lower one quickly accelerated upward causing the upper plate to move as well. Since modeling the effects of pressure are beyond the capacity of ConWep, the compromising solution to maintain a degree of accuracy for injury results is to place the

feet close to the protective plate. The proximity of the dummy to the protective plate ideally replicates the injuries caused by the floor plate accelerating into the cabin.

The legs of the ATD are left in their default position. The thighs are horizontal and the lower legs rest at a natural right angle. The arms are rotated to 90°, the common position for crash and blast testing. The wrists and hands maintain the default straight position.

Lastly, contacts between the ATD and seat as well as the feet and plate are defined. Rigid contacts come from LS-DYNA tutorials (LSTC, 2010). The automatic surface to surface contacts include combinations of values from blast tutorials (RCC, 2010) and other DRDC models (Tan et al., 2010d). The static coefficient refers to the friction between two stationary objects, while the dynamic coefficient applies when a body is in motion relative to the other. The transition between static and dynamic coefficients is described by the exponential decay coefficient. Since the static and dynamic properties are the same, the decay coefficient can be set to the default value of zero. Frictional contact stress is limited based on the yield strength of the material through the coefficient of viscous friction. The viscous damping coefficient refers to friction in an oscillating system, input as a percentage of critical damping. These properties are presented in Table 5.

Table 5:

Contact definitions

Property	ATD and Seat	ATD and Plate
Type	Rigid	Surface to Surface
Static Coefficient of Friction	0.2	0.3
Dynamic Coefficient of Friction	0.2	0.3
Coefficient of Viscous Friction	0	0.5
Viscous Damping Coefficient	0	90 %
Exponential Decay Coefficient	0	0
Unloading Stiffness	0.75	NA

Even when a dummy is incorporated into the system, the symmetry of the device is still present. Most armored vehicles have seats along the sides of the cabin, and rotating the quarter-plate and dummy about the main axes represents four occupants equally spaced along the sides of the cabin.

4.3 Three Optimized Plate Designs

Three additional plates with shapes determined by different optimization algorithms were developed and modeled by Tan et al. (2010d). The fourth plate, the control plate, is the flat one described by Williams et al. (2003). The four plates are depicted in Figure 4. The independent variable during testing is the shape of the plate, while the dependent variables are the injuries induced. The injuries associated with each shape are compared against each other and against those from the control flat plate to determine which protects best against leg injuries. The most important conclusion is which variable of the plate deformation contributes most to injury. For example, the relationship between the velocity of the protective plate and injury severity is evaluated.

The first plate, also known as the Displacement Basis plate, is a 1-D optimization technique that varies only the radius of the shell. The result is a parabolic curve. The design of the second plate utilizes the HCA method proposed by Tovar et al. (2006). This method iteratively evaluates nodal accelerations, compensates for error, and updates coordinates until it reaches convergence. The HCA method has many variables, so the resultant plate has many bends and is defined by many curves. The last optimized plate is based on a Gaussian investigation with two design variables, depth of plate and width of distribution. In this case, the width is maximized to match the width of the entire visible plate. All plates have the control parameter that the maximum depth of the plate could be no more than 200 mm below the flat plate position. This parameter is based on external design requirements, such as cabin height and ground clearance.

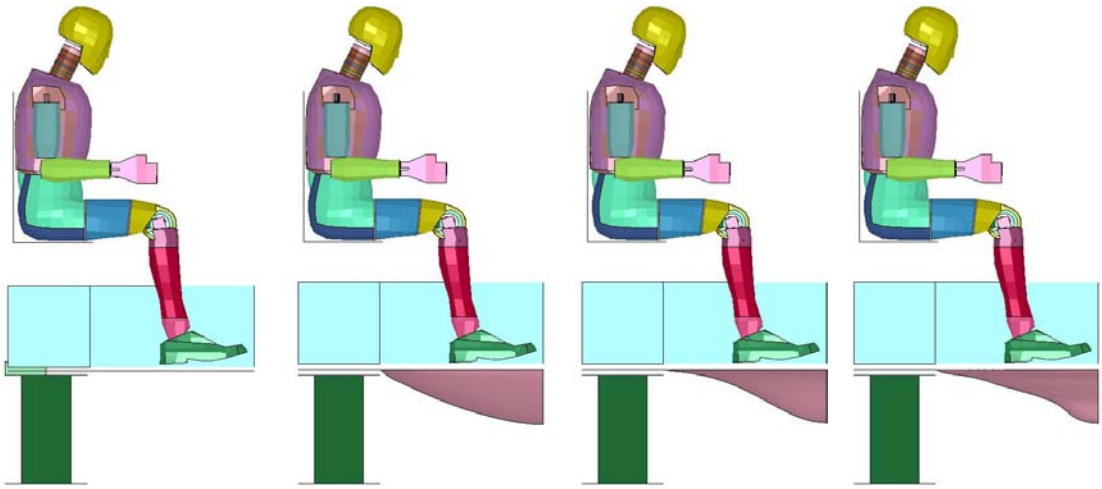

A) B) C) D)

Figure 4: Plate designs: A) Flat, B) Displacement Basis, C) Gaussian, D) HCA

4.4 Replacing Aluminum with Armored Steel

In a final trial, the unmodified, flat plate was replaced with an RHA steel plate of the same dimensions. The properties for these metals are listed in Table 4. This test determines the amount of extra protection offered by steel, a stronger material. It also weighs the advantages of additional protection versus the drawbacks of additional weight.

CHAPTER 5:

BLAST MODEL

5.1 ConWep Model

Blasts are modeled in LS-DYNA using an imbedded function called ConWep, short for Conventional Weapons. This loading function requires the user to input mass of TNT, location in Cartesian coordinates, and type of burst – spherical or hemispherical. The user then selects the surface or surfaces where the blast load is applied. ConWep mathematically calculates the force on the selected surface over a period of time based on mass of TNT, distance from blast, and angle of incidence. It incrementally updates the pressure load on the selected surface over a set time interval. It does not account for the effects of the soil over a buried bomb or the pressure wave that travels through the surrounding air. These drawbacks cause ConWep to underestimate damage and deformation. An alternative to ConWep is the Arbitrary Lagrangian Eulerian method (ALE), which can simulate the compound effects of pressure, air, and soil. While it is a more realistic modeling method, it is vastly more complex and costly and not a feasible option for the scale of this research.

5.2 Validation

In May 2000, Williams and his team in Valcartier, Canada conducted field trials to validate the DRDC plate model. They studied numerous virtual and physical tests. Their results demonstrated the effectiveness of using a virtual model to accurately represent the DRDC plate model in a blast test.

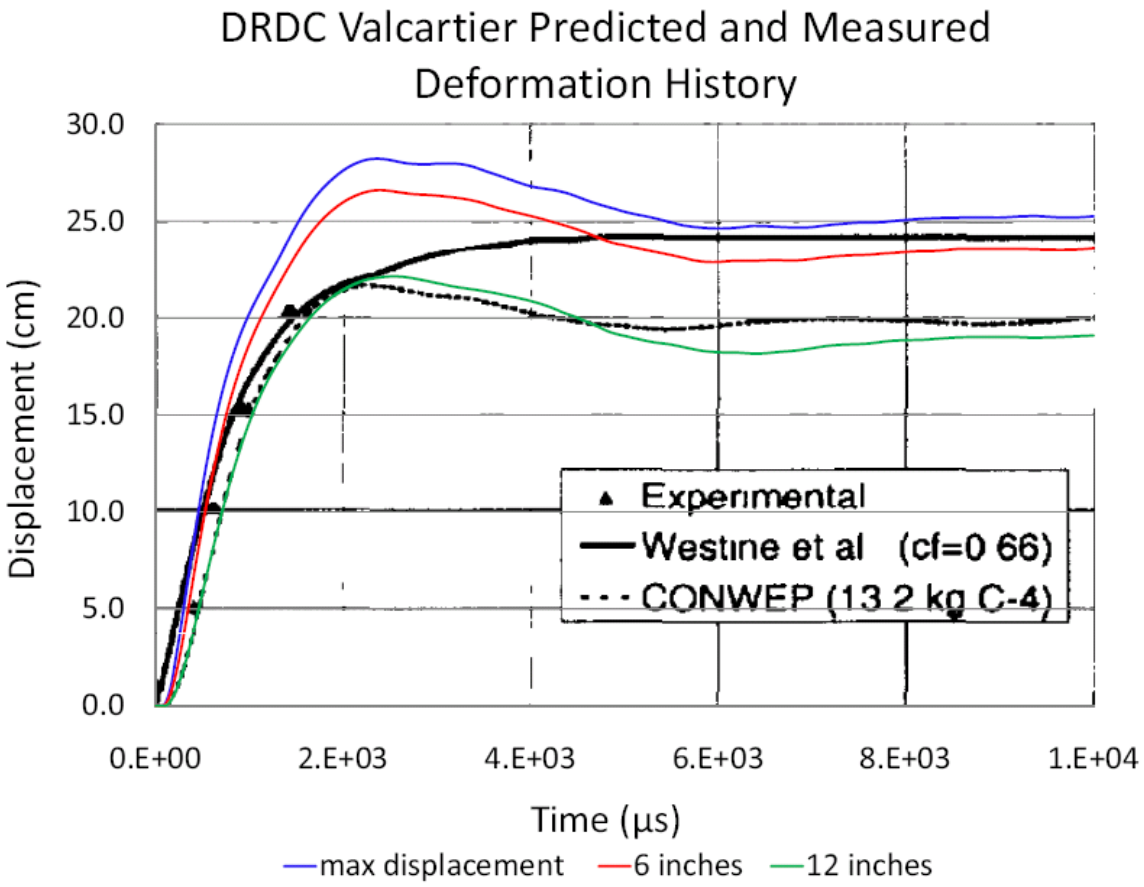

Figure 5: Validation of ConWep model (Williams et al., 2003)

The green line in Figure 5 represents the ConWep model of the DRDC plate used in this research without an ATD. The dashed line stands for the ConWep model from Williams et al. (2003). Both ConWep trials were simulated using LS-DYNA. The solid black line represents a different approach to virtually simulating a blast under the DRDC

plate. Westine et al. (1985) developed a program for the US Army TACOM that evaluated the impulse at numerous points. Notably, this model took into account burial depth and soil density. The triangles are experimental data from an actual blast test performed by the team in Valcartier. The displacement was measured by a set of piezo-pins located across the plate. The data from these four trials were measured from a point 12 in away from the center of the plate.

Clearly, the four trials measure similar results. Though the plates in each trial settle to slightly different final displacements, the initial rising motion is very similar. The rising period is the most important for injury assessment since this is when the plate would strike the feet of an occupant. This implies that ConWep, despite its limitations, actually closely mimics the behavior of an actual DRDC plate under blast loading. Also, it can produce just as reliable results as more complicated FEM programs. ConWep is validated as an appropriate model for a blast under a DRDC plate. The movement of the plate under real blast loads can be easily replicated without detonating actual mines.

5.3 Location of Blast

The blast location is kept constant for all trials. It is located exactly 1 m below the center of the full plate or the corner of the quarter plate. This location is based on actual vehicle specifications. Figure 6 depicts a typical light armored vehicle. The back section of the vehicle seats up to four occupants. The floor panel is around 0.88 m above ground level. An additional 0.12 m was added to this height to include burial depth of blast and extra height from floor panels and boots. From Williams et al. (2003), charges

are commonly buried 5 to 20 cm deep, so adding 10 cm for burial depth and 2 cm for boot thickness is appropriate. Therefore, 1 m is a realistic assumption for the distance between the plate and the charge.

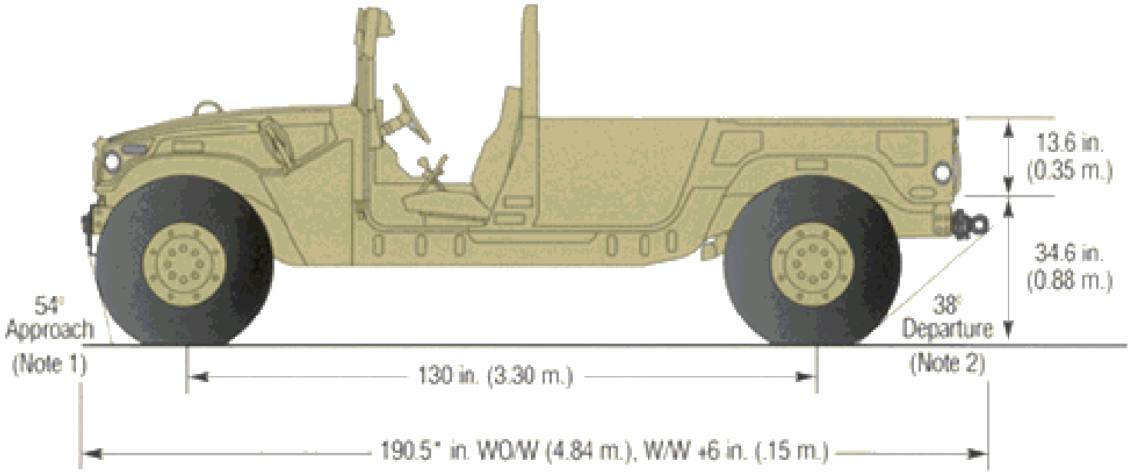

Figure 6: Humvee specifications (AM General, 2009)

5.4 Mass of Blast

The mass of the charge is also kept constant at 15 kg. Average blasts can vary from 5 kg to 15 kg (HFM-090 Task Group 25, 2007). ConWep consistently underestimates blast loading since it does not take the exacerbating effects of soil into account. Therefore, the mass of TNT entered into the ConWep function should be increased by a factor of two to three (Brill et al., 2007). Assigning the mass to be 15 kg would then represent an actual blast from about 5 to 7.5 kg of TNT. However, actual vehicles have an additional lightweight floor panel that separates the interior cabin from the blast protection plate. The additional layer would provide some blast protection. The results gathered in this research with only one panel between the blast and ATD would

represent injuries worse than realistic, injuries that would be more characteristic to a larger blast. The overestimation of blast effects from the lack of additional floor panels would cancel with the underestimation of the ConWep function. Depending on the amount of cancellation between those two effects, a virtual 15 kg could model an actual blast between 5 and 15 kg. This precisely fits the average range from literature.

CHAPTER 6:

SIMULATION AND RESULTS

6.1 Visual Representation of Results

LS-PrePost processes the numerical data output from LS-DYNA into both visual and graphical components. The protection offered by the four plates can be visually assessed using the three dimensional models in LS-PrePost. Snapshots depicted in Figure 7 demonstrate the displacement and rotation of the legs 5 and 10 ms after the blast.

Observations from these snapshots can provide insight into the injuries caused during the blast event. First, the legs that displace a greater distance during the same period of time likely incur more severe injuries. Also, both feet over the Displacement Basis plate and the right foot over the HCA plate do not significantly move from their initial positions. Lastly, the feet can rotate about the ankle, exemplified in the left foot over the HCA plate. The moment caused by this rotation may play a role in leg injury. These observations are quantified in the following sections.

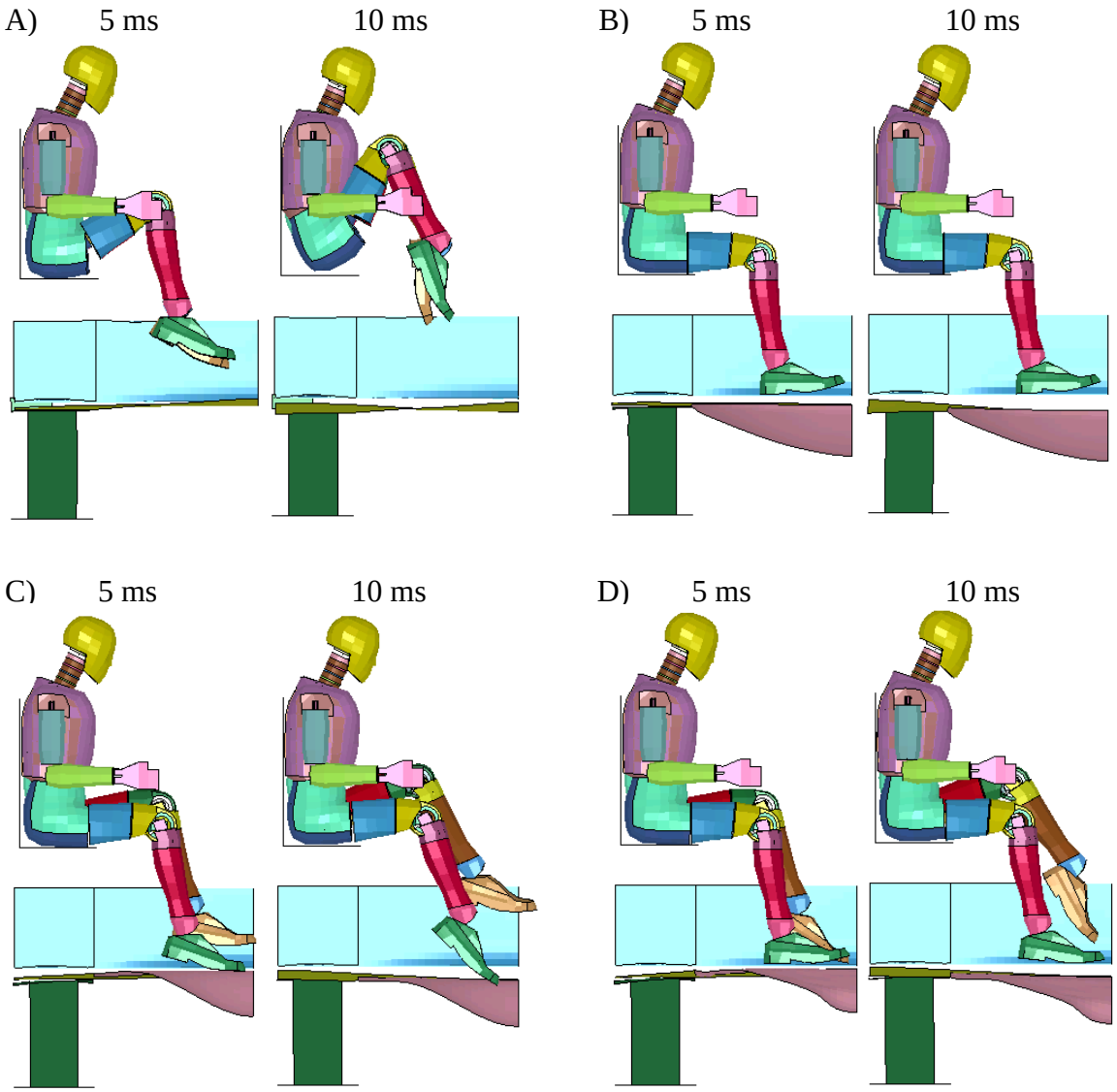

Figure 7: Blast event snapshots: A) Flat, B) Displacement Basis, C) Gaussian, D) HCA

6.2 Femur Injury

The axial forces across the femur are recorded in Figure 8. The red line marks the critical injury value of 10 kN in compression where AIS 2+ injuries are likely. The most important data are the minimum points. Clearly, the occupant over the flat plate breaks

both femurs and faces possible amputations. The occupants over the Gaussian and HCA plates likely sustain severe injuries in their left femurs but only mild injuries in their right legs. The occupant over the Displacement Basis plate faces no femoral loading due to the acceleration of the plate into the cabin.

Femurs can withstand higher compressive forces than tensile forces. In the flat plate trial, the tensile forces reach compressive limits, thus increasing the likelihood for even further injury. Tensile forces can be responsible for dislocation or amputation, both possibly fatal injuries. The other trials do not face significant tensile forces.

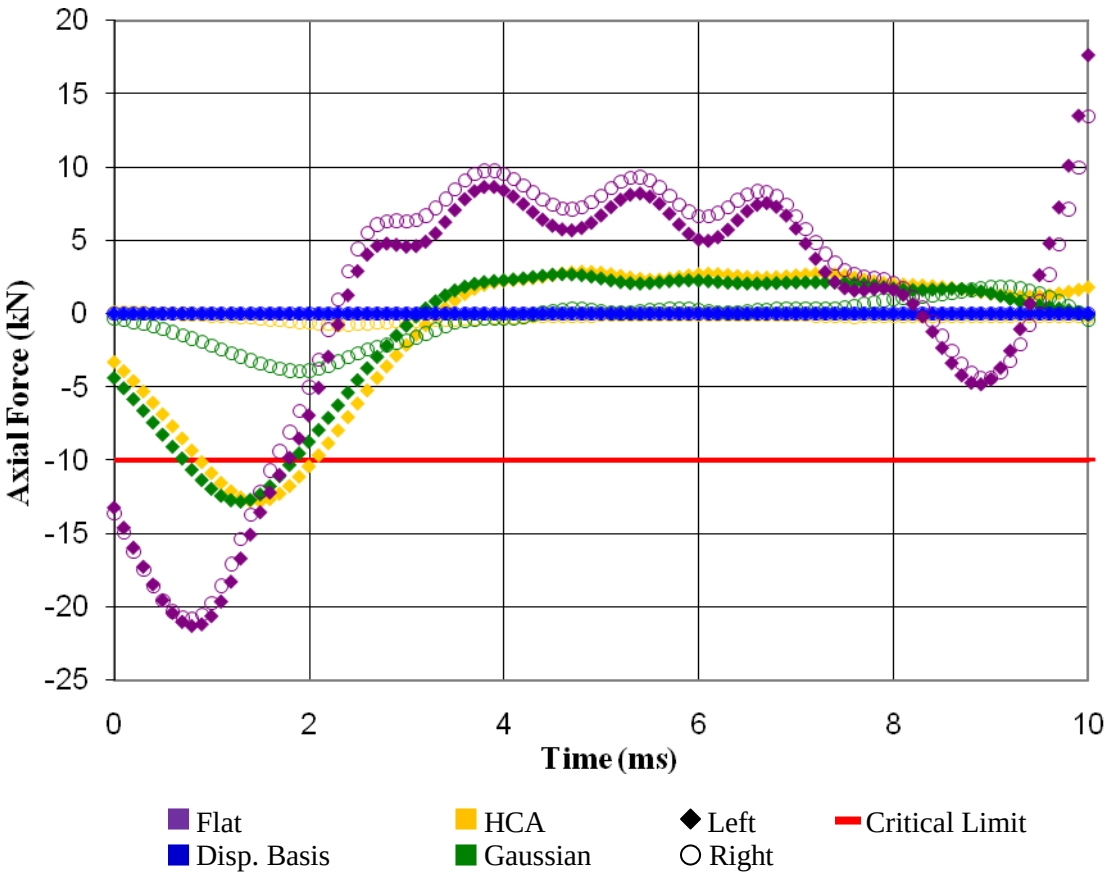

Figure 8: Femur axial force

6.3 Tibia Injury

Corrected tibia moments and axial forces are measured in LS-PrePost. Figure 9 depicts these values. The red line at an index value of one marks the critical tibia index where severe injuries are likely. The occupants in the flat, Gaussian, and HCA plate trials sustain severe and possibly life threatening injuries. The right tibia in the HCA trial may be only mildly fractured since the index value does not exceed one. Again, the Displacement Basis occupant does not register any loading.

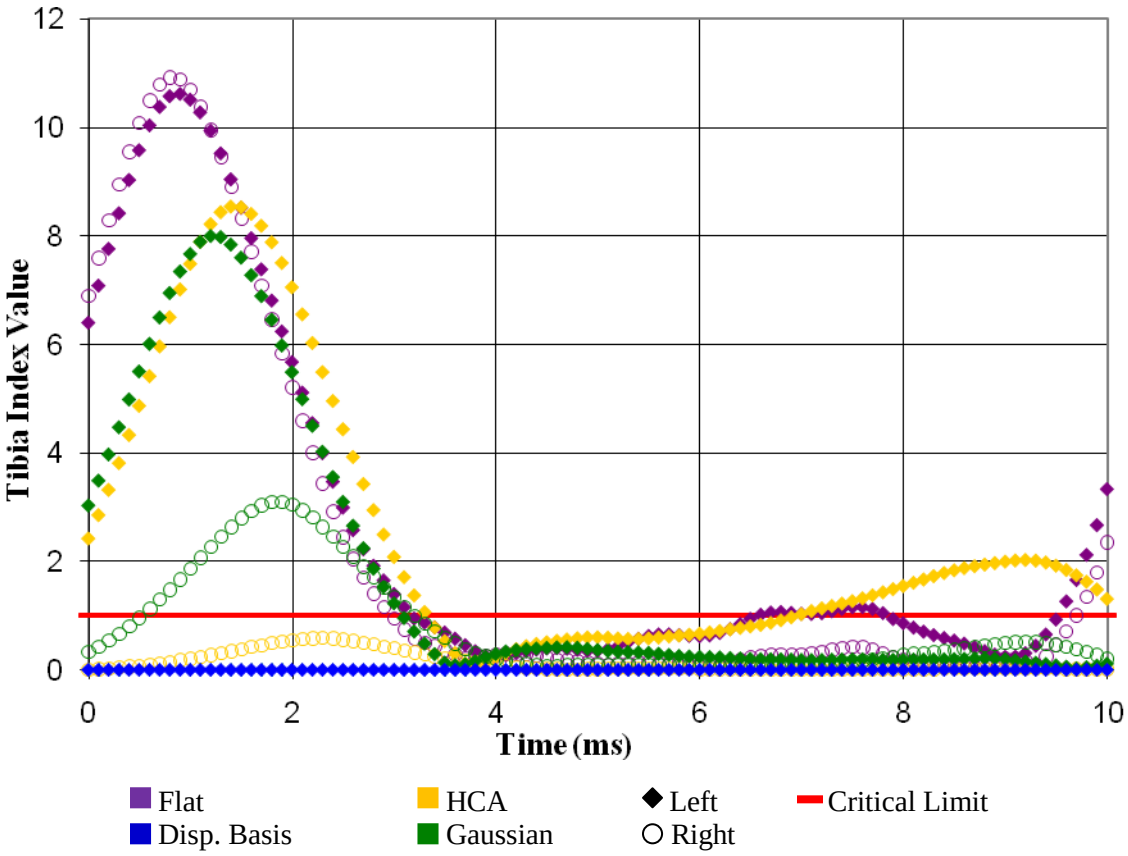

Figure 9: Tibia indices

6.4 Cabin Penetration at Heel Reference Points

The cabin penetration distances at the heel reference points are compared in Figure 10. The flat plate position is considered the zero reference point or the bottom boundary of the cabin. The heel reference points were selected to study since they directly contact the dummy. In general, the simulations have similar characteristics, but they reach different maxima. The Displacement Basis plate had the lowest maxima, but it also was the furthest from the feet at time t=0. However, the magnitude of the difference between the maximum penetration and the position at time t=0 is the least for the Displacement Basis plate. The HCA, Gaussian, and flat plate displace a greater distance from their initial position while also having more penetration into the cabin.

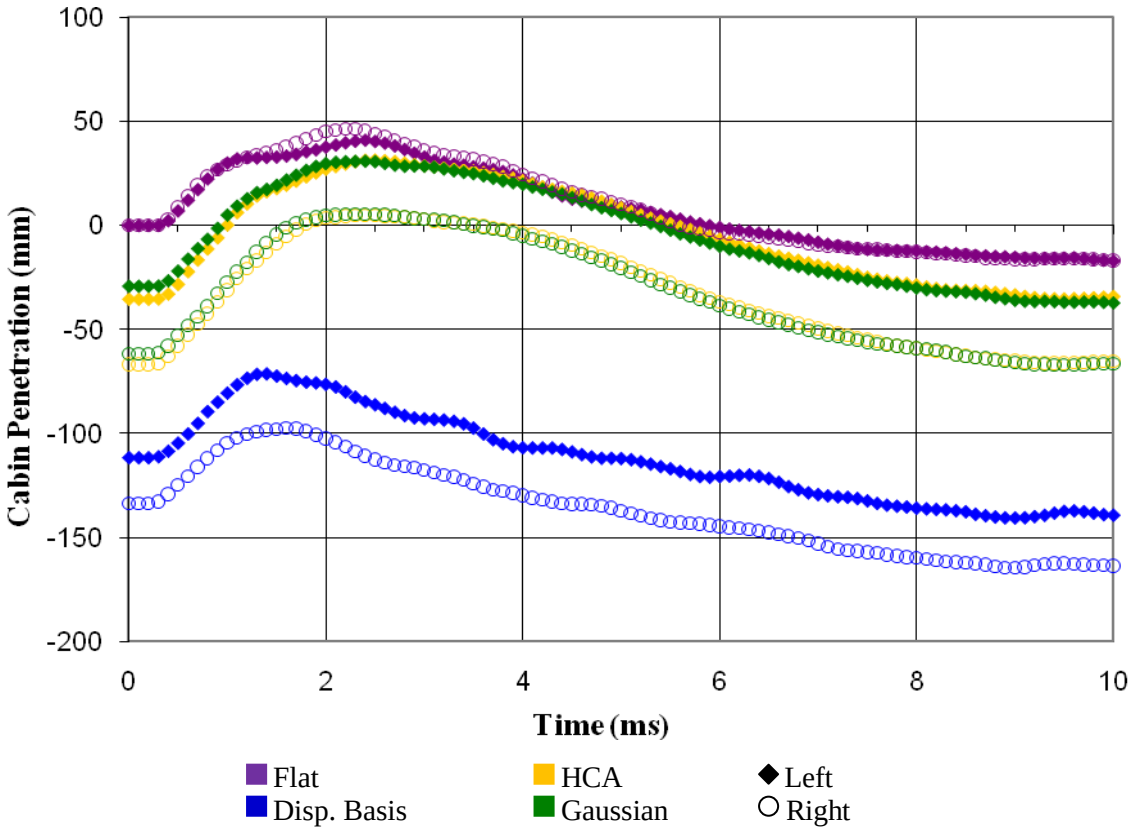

Figure 10: Cabin penetration at heel reference points

6.5 Protective Panel Velocity at Heel Reference Points

The velocity of the heel reference points is recorded in Figure 11. The larger points represent the velocities at the times when the heel reference points come into contact with the heels of the Hybrid III ATD. The plate never contacts the feet for the Displacement Basis trial. Only the first three milliseconds are recorded since the plates do not contact the feet after this time.

The plot has a few notable characteristics. First, the flat plate hits the feet with the highest velocity of the four simulations. Also, the HCA and Gaussian plates both hit the feet at a higher speed for the left foot than the right foot.

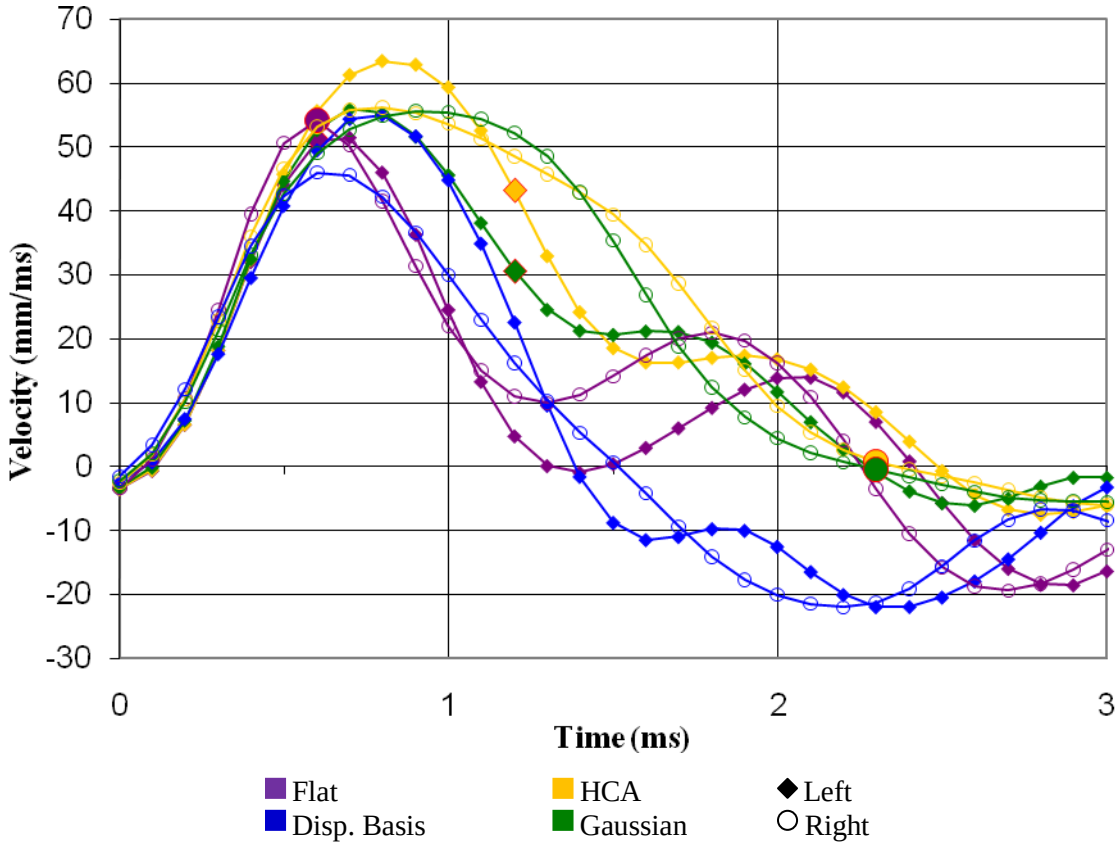

Figure 11: Velocity of Heel Reference Points

6.6 Protective Panel Acceleration at Heel Reference Points

The acceleration of the heel reference points is displayed in Figure 12. Again, the larger data points are the accelerations at the time of impact with the ATD feet. Each plate's acceleration has an irregular sinusoidal shape. The acceleration was deemed the most important variable to study during blast tests by Tan et al. (2010d) and was minimized during the optimization processes.

The plot had numerous unexpected characteristics. The highest acceleration is by the flat plate for the left foot, but the flat plate also has the lowest acceleration at impact with the right foot. The HCA and Gaussian plates have similar acceleration histories, but impact the feet while decelerating.

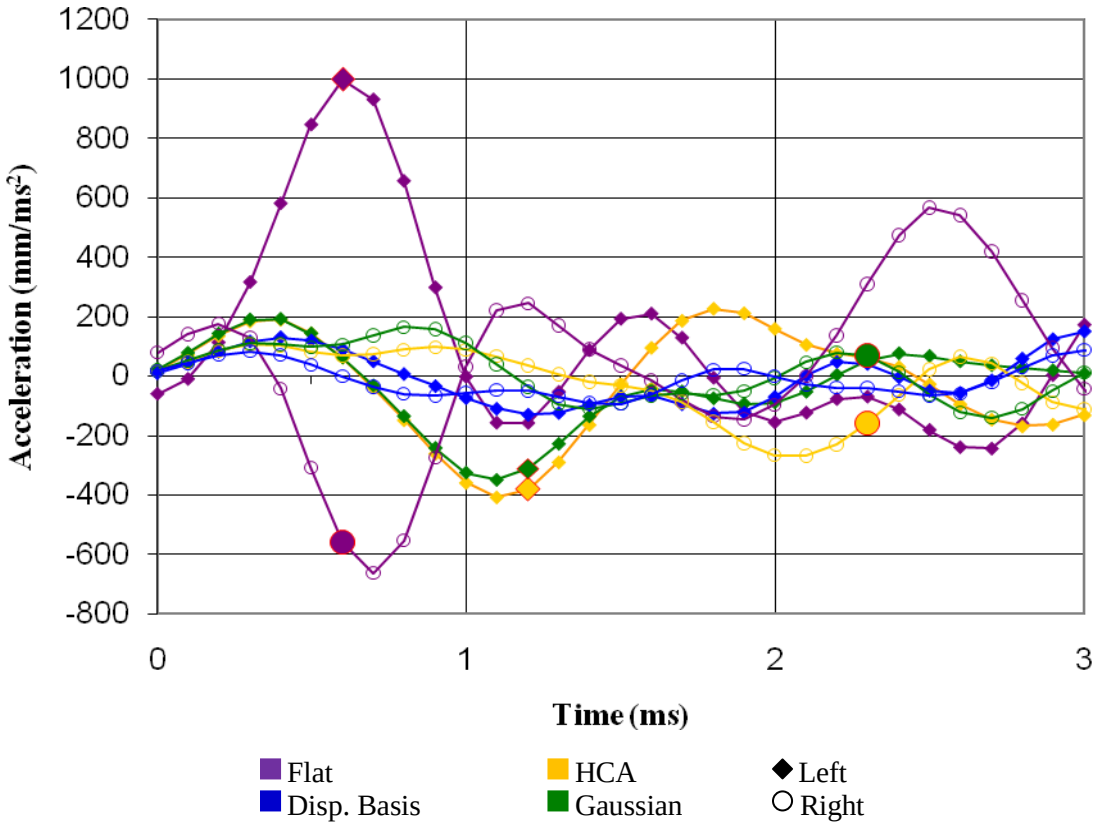

Figure 12: Acceleration of heel reference points

6.7 Steel versus Aluminum Plate

The steel plate reduces axial forces in the femur by nearly 50 % when using a flat plate, as depicted in Figure 13. Again, the red line refers to the 10 kN compressive critical limit of the femur. Steel, however, has one major drawback. Using a steel plate instead of an aluminum plate causes a threefold increase in weight. For three times the weight, axial forces on the femurs are only cut by a factor of two. Whereas, an aluminum plate shaped in the optimum design can dramatically decrease occupant loading with only minimal additional weight. Light armored vehicles may not be able to support the heavy weight of a steel plate. Therefore, an aluminum plate, shaped to the optimal design for protection, is a more reasonable supplement to protect traditional vehicles.

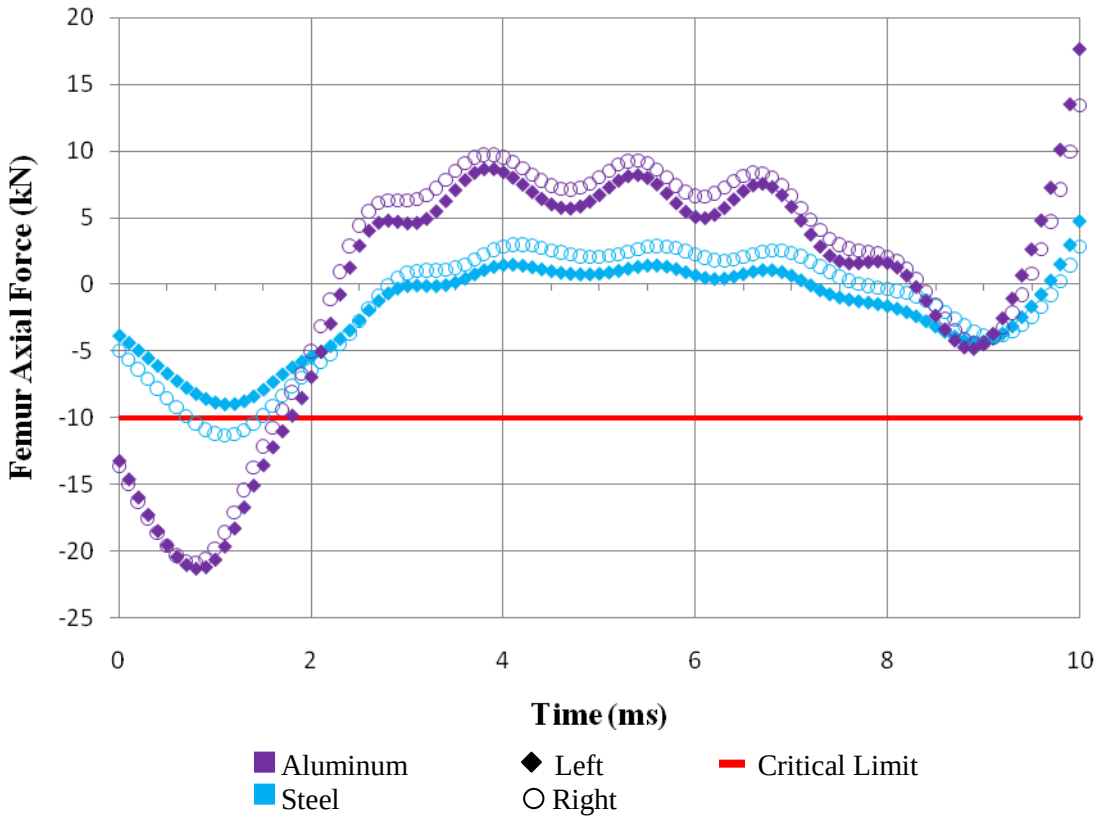

Figure 13: Steel versus aluminum femur axial forces

CHAPTER 7:

CONCLUSIONS

Cabin penetration is the best predictor of injury in this experiment. A positive correlation exists among penetration and loading on the occupant's legs. Trends in the data exemplify this relationship. For one, the right leg over the flat plate sustains higher tensile forces and a higher maximum tibia index than the left leg. Notably, the part of the hull under the right foot deforms farther into the cabin than that under the left foot. Another example is the order of ascending injury for the right leg and the order of ascending penetration under the right foot are the same - Displacement Basis, HCA, Gaussian, and flat plate. This demonstrates that as cabin penetration increases so does the measured indices.

In order to decrease penetration, displacement has to be minimized. The reference points of the Displacement Basis plate displace the smallest distance from their original location than any other plate. In this way, the Displacement Basis plate retains its concave shape even during blast loading. Whereas, the HCA and Gaussian plates buckle up and lose their shape, which results in large displacements and large penetration distances. The buckling is due to the snap-through effect. This occurs when the bowl-like shape of the plate is distorted so the center of the plate buckles upward more than the

surrounding material. The results demonstrate that the snap-through effect is very dangerous for the occupants. A plate that retains its shape offers more protection.

The velocities of the heel reference points at the time of impact have only a weak correlation to injury. It is less accurate as an indicator of injury than cabin penetration. For example, it does not account for why the right leg over the Gaussian plate is subjected to significantly higher loadings than those produced by the HCA plate. Not all plates have the same relation between velocity at impact and injury, which decreases the accuracy of plate velocity as a predictor of injury.

Both overall acceleration and acceleration at the time of impact do not appear to influence the severity of injury during these specific blast simulations. Though unexpected, it explains why the Displacement Basis plate performs better than the more complex HCA plate in this experiment. More trials with different blast arrangements would need to be conducted to fully understand the relationship between plate acceleration and injury.

The results of these simulations suggest cabin penetration is an appropriate tool for assessing injuries. Injury is less for occupants over plates that have less cabin penetration. For future protection designs, cabin penetration should be a variable of interest. Also, plates without snap-through effects trigger fewer injuries since they retain their shape and have minimum cabin penetration. The Displacement Basis plate keeps its parabolic shape and thus offers more protection than a flat plate.

The limitations of blast computer simulations as previously discussed introduce uncertainty. The main shortcoming of the ConWep model is that it cannot model compressed air. The rapid acceleration of the protective plate would compress air, which

in turn could move other components of the vehicle. This alone would have the potential to cause damage even if the plate itself does not contact the feet. However, this limitation can be overcome, resulting in useable results. Increasing the mass of blast material can mimic the effects of overpressure from a smaller blast.

Also, the consistency of the set-up in each test means the results are accurately compared since limitations similarly affect each simulation. The data therefore is best used as a comparative analysis that recognizes trends not exact numerical values. The simulations do not precisely demonstrate the literal injuries sustained by an occupant, but they do offer insight into the best ways to protect occupant legs during a vehicular blast.

REFERENCES

AM General (2009) Dimensions: A2 Series HMMWV (Humvee). *AM General LLC - Mobility Solutions for the 21st Century* (accessed August 2, 2010).

Bellis, M. (2010) History of Crash Test Dummies-Sierra Sam. *Inventors* (accessed June 5, 2010).

Brill, A., B. Cohen & P.A. DuBois (2007) Simulation of a Mine Blast Effect on the Occupants of an APC. *6th European LS_DYNA Users' Conference*. RAFAEL Ballistic Center, Israel.

Chichester, C., C. Bass, B. Boggess, M. Davis, E. Sanderson, G. Di Marco, W. Andrefsky & W.B. Hess (2001) A Test Methodology for the Assessing Deming Personal Protective Equipment (PPE). *Humanitarian Demining*, 1, 20-55.

Defense Manpower Data Center (2010) Global War on Terrorism by Reason October 7, 2001 – July 31, 2010 (accessed August 5, 2010).

Durocher, R. (2003) JOWZ Valley Mine Strike Preliminary Technical Report: Investigation of a Mine Strike Involving Canadian Troops in Afghanistan. *Defence Research & Development Canada – Valcartier*, 1, 1-31.

Eisler, P., B. Morrison & T. Vanden Brook (2007) Pentagon balks at pleas for safer vehicles. *USA Today*.

Grujicic, M., G. Arakere, W.C. Bell & I. Haque (2009) Computation investigation of the effect of up-armouring on the reduction in occupant injury or fatality in a prototypical high-mobility multi-purpose wheeled vehicle subjected to mine blast. *Proceedings of the Institution of Mechanical Engineers Part-D: Journal of Automobile Engineering*, 223, 903-920.

Guha, S., D. Bhalsod & J. Krebs (2008) LSTC Hybrid III Dummies Positioning & Post-Processing. *LSTC Michigan*.

HFM-090 Task Group 25 (2007) Test Methodology for Protection of Vehicle Occupants against Anti-Vehicular Landmine Effects. *NATO Research and Technology Organization*, 4.1-4.14, I.1-I.18.

Insurance Institute for Highway Safety (2009) Frontal Offset Crashworthiness Evaluation. *Guidelines for Rating Injury Measurements*.

Kuppa, S., J. Wang, M. Haffner & R. Eppinger (2001) Lower Extremity Injuries and Associated Injury Criteria. *National Highway Traffic Safety Administration Proceedings of the 17th International Technical Conference on the Enhanced Safety of Vehicles*, Amsterdam.

Livermore Software Technology Corporation (2010) Tutorials. *LS-PrePost: Online Document* (accessed June 5, 2010).

Mayorga, Maria A. (1997) The Pathology of Primary Blast Overpressure Injury. *Toxicology*, 121, 17-28.

Mertz, H.J. (1993) Anthropometric Test Devices. *Accidental Injury: Biomechanics and Preventions*, Springer-Verlage, New York.

Nelson, J.K Jr., P.J. Waugh, A.J. Schweickhardt (1996) Injury Criteria of the IMO and the Hybrid III Dummy as Indicators of Injury Potential in Free-Fall Lifeboats. *Ocean Engineering*, 23 (5), 385-401.

Noureddine, A., A. Eskandarian & K. Digges (2002) Computer Modeling and Validation of a Hybrid III Dummy for Crashworthiness Simulation. *Mathematical and Computer Modeling*, 35, 885-893.

Research Computing and Cyberinfrastructure (2010). Setting up Explosive Blast Loads in LS-DYNA. *High Performance Computing*, Penn State (accessed June 23, 2010).

Rupp, J.D., M.P. Reed, N.H. Madura, S. Kuppa, & L.W. Schneider (2003) Comparison of knee/femur force-deflection response of the Thor, Hybrid III, and Human Cadaver to dynamic frontal-impact knee loading. *National Highway Traffic Safety Administration*, Paper No. 160.

Stuhmiller, J.H. (2008) *Blast Injury: Translating Research into Operational Medicine*, Borden Institute.

Tan, H., J. Goetz, A. Tovar, and J.E. Renaud (2010a) HCA approach to topography design optimization of a structure for fluid structure interaction. *In Proceedings of the 51st AIAA/ASME/ASCE/AHS/ASC Structures, Structural Dynamics, and Material Conference*, Orlando, Florida.

Tan, H., J. Goetz, A. Tovar, J.E. Renaud (2010b) Simultaneous Topography Optimization of a Vehicle Hull and Topology Optimization of the Assembly Interface for Blast Mitigation. *2010 Ground Vehicle Systems Engineering and Technology Symposium (GVSETS)*, Troy, Michigan.

Tan, H., J. Goetz, A. Tovar, J.E. Renaud (2010c) Validation of Computational Fluid Structure Interaction Models For Shape Optimization Under Blast Impact. *ASME 2010 International Design Engineering Technical Conferences & Computers and Information in Engineering Conferences (IDETC/CIE)*, Montreal, Canada.

Tan, H., J. Goetz, A. Tovar & J.E. Renaud (2010d) Vehicle Hull Shape Optimization for Minimum Deformation under Blast Loading. Document submitted to *International Journal of Impact Engineering.*

Tovar, A., N.M. Patel, G.L. Neibur, M. Sen & J. Renaud (2006) Topology Optimization Using a Hybrid Cellular Automata Method with Local Control Rules. *ASME Journal of Mechanical Design*, 128 (6), 1205-1216.

Van der Horst, M.J., C.K. Simms, R. van Maasdam & P.J.C. Leerdam (2005) Occupant Lower Leg Injury Assessment in Landmine Detonations Under a Vehicle. *IUTAM Proceedings of Impact Biomechanics: From Fundamental Insights to Applications*, 41-49.

Welbourne, E.R. & N. Shewchenko (1998) Improved Measures of Foot and Ankle Injury Risk from the Hybrid III Tibia. *Proceedings of the 16th International Technical Conference on the Enhanced Safety of Vehicles*, 98-S7-O-11, 1618-1627.

Wikipedia (2010) Crash Test Dummy. *Wikipedia* (accessed June 2, 2010).

Williams, K., S. McClennan, R. Durocher, B. St-Jean & J. Tremblay (2003) Validation of a Loading Model for Simulating Blast Mine Effects on Armored Vehicles. *7th International LS-DYNA Users Conference*, 35-34.